

Electromagnetic waves in a metal near cyclotron resonance in an oblique magnetic field

Yu. I. Man'kov, L. M. Gorenko, and R. G. Khlebopros

L. V. Kirenskii Physics Institute, Siberian Division, USSR Academy of Sciences

(Submitted 15 May 1979)

Zh. Eksp. Teor. Fiz. 77, 2142-2152 (November 1979)

Weakly damped electromagnetic waves propagate in a normal metal placed in a magnetic field near cyclotron resonance and inclined to the surface of the metal. The waves propagation makes an angle with the magnetic field. It is shown that three waves exist near the attenuation minimum due to the vanishing of the Landau damping. One wave was investigated before for limiting cases, and the other two were obtained for the first time ever. These two waves have opposite polarizations. The frequency of the right-polarized wave is lower than that of the cyclotron resonance, while that of the left-polarized one is higher. The dependence of the natural frequency, of the polarization, and of the damping on the magnetic field H , on the wave vector k , and on the angle between H and k was investigated for all the waves. A relation between the waves near the cyclotron resonance and low-frequency excitations, on the one hand, and the classical discrete spectrum, on the other, is demonstrated.

PACS numbers: 41.10.Hv, 76.40.+b

INTRODUCTION

Electromagnetic waves propagating in metals and close in frequency to cyclotron resonance were first considered theoretically by Kaner and Skobov.¹ These waves, named cyclotron waves, propagate perpendicular to the applied constant magnetic field and are due to the presence in the metals of cyclotron resonance in a strong ($\nu \ll \Omega$) magnetic field parallel to the sample surface²; ν and Ω are the collision frequency and the cyclotron frequency of the conduction electrons. Cyclotron waves in metals have been the subject of many studies, the results of which are contained in many books^{3,4} and reviews.⁵⁻⁸ None the less, cyclotron waves continue to attract attention.⁹⁻¹⁶

Cyclotron resonance is observed also in a magnetic field inclined to the sample surface. This phenomenon, however, is more complicated than in a field parallel to the surface, and although the effect of the inclination of the magnetic field on the cyclotron resonance was investigated even in the first studies of this phenomenon,¹⁷ a complete theory of cyclotron resonance in an oblique magnetic field was developed only recently.^{18,19} As to weakly damped electromagnetic waves near cyclotron resonance in an oblique magnetic field, they have been studied only little. We know of only two papers dealing with these waves. Blank and Kaner²⁰ obtained the spectrum and the damping of such waves under the assumption that the spread of the diameters of the effective electrons is characterized by a parameter w and that the case considered corresponds to $|w| \ll 1$. Aronov and Kaner¹⁸ solved the problem for the opposite limit $|w| \gg 1$. In both papers the waves considered had a length $2\pi k^{-1}$ much less than the cyclotron radius R of the conduction electrons; the surface impedance was found to have singularities due to the existence of weakly damped waves. The inclination angle φ between the magnetic field and the sample surface was assumed small, i.e., the waves considered propagated at an angle close to $\lambda/2$ with the magnetic field.

Consideration of cases with limiting values of the

parameter w leads to additional limitations. Thus, the condition $|w| \ll 1$ limits the frequency ω of the electromagnetic wave to a value close to the frequency $N\Omega$ of the cyclotron resonance¹⁸ (N is an integer). The condition $|w| \gg 1$ (Ref. 20) yields results that are valid for very short waves, since the inequality $|w| \cdot (kR)^{-1/2} \ll 1$ must be satisfied in addition to the condition $|w| \gg 1$. By lifting the restrictions on w we can consider waves in a wider range of fields, frequencies, and wave vectors.

In addition to the waves near cyclotron resonance, there are known²¹⁻²³ also low-frequency ($\omega \ll \Omega$) waves that propagate at an angle close to $\pi/2$ to the magnetic field, and are classified⁸ as helicon waves. A distinguishing feature of these waves is the discreteness of their spectrum, due to the vanishing of the Landau magnetic damping at a definite ratio of the conduction-electron cyclotron radius to the wave vector. The similarity of their propagation conditions make these two types of wave close in many respect, so that it is also of interest to trace the connection between them and to obtain general expressions for the characteristics of the waves.

DISPERSION EQUATION AND CONDUCTIVITY TENSOR

To describe the propagation of an electromagnetic wave in an unbounded metal we use the system of Maxwell's equations

$$i[k \times h] = 4\pi c^{-1} j, \quad (1)$$

$$[k \times E] = \omega c^{-1} h. \quad (2)$$

Here E is the alternating electric field, h is the high-frequency part of the magnetic field $E, h \propto e^{i(kr - \omega t)}$, H is the external constant magnetic field, j is the current density, and k is the wave vector. We neglect the displacement vector in Maxwell's equations, in which case it follows from (1) that

$$kj = 0, \quad (3)$$

which is analogous to the condition for the electric

quasineutrality of the metal.

We choose the coordinate system xyz such that the z axis is parallel to the magnetic field \mathbf{H} and the x axis is perpendicular to the plane of \mathbf{H} and \mathbf{k} . In addition, we introduce also the coordinate frame $x\eta\zeta$, in which the ζ axis is parallel to \mathbf{k} (Fig. 1) and makes an angle $\pi - \varphi$ with the y axis. Substituting (2) in (1) and eliminating with the aid of (3) the electric-field component E_z that is longitudinal relative to \mathbf{k} , we reduce Eqs. (1) and (2) to a system of linear homogeneous equations for the transverse components E_x and E_η . Equating the determinant of this system to zero we get the dispersion equation

$$16\pi^2 (\delta_{zz}\delta_{\eta\eta} - \delta_{z\eta}\delta_{\eta z}) \omega^2 + 4\pi i k^2 c^2 (\delta_{zz} + \delta_{\eta\eta}) \omega - k^4 c^4 = 0, \quad (4)$$

$$\delta_{\alpha\beta} = \sigma_{\alpha\beta} - \sigma_{\alpha i} \sigma_{i\beta} / \sigma_{ii}. \quad (5)$$

Here $\sigma_{ij} \equiv \sigma_{ij}(\mathbf{k}, \mathbf{H}, \omega)$ are the Fourier components of the conductivity tensor. The indices α, β and i, j take on respectively the values x, η and x, η, ζ . The dispersion equation (4) was first obtained by Kaner and Skobov²¹ and describes an electromagnetic wave propagating at an angle to the magnetic field.

In the case of an isotropic and quadratic electron dispersion, the following expression holds for the elements of the conductivity tensor⁵

$$\sigma_{ij} = \frac{3n_0 e^2}{4\pi m \Omega v^2} \int_0^\pi d\theta \sin \theta \int_0^{2\pi} d\tau v_i \int_{-\infty}^{\infty} d\tau' v_j \exp \left[\int_{\tau'}^{\tau} d\tau'' \frac{v - i\omega + ikv}{\Omega} \right], \quad (6)$$

where n_0 is the conduction-electron density, e , m and v are respectively the charge, effective mass, and Fermi velocity of the electron, and θ and τ are the polar and azimuthal angles of the velocity vector. The polar axis coincides with the z axis.

Expressing the electron velocity components $v_{x,\eta,\zeta}$ in terms of $v_{x,y,z}$, we obtain in analogy with Kaner and Skobov⁶ for the elements of the conductivity tensor

$$\sigma_{ij} = \frac{3n_0 e^2}{2m} \sum_{N=-\infty}^{\infty} \int_0^\pi d\theta \frac{\sin \theta \omega_i \omega_j^*}{v - i(\omega - N\Omega - k_z v \cos \theta)}, \quad (7)$$

where

$$\begin{aligned} w_x &= -iJ_N'(x) \sin \theta, & w_\eta &= -\left(\cos \theta \cos \varphi - \sin \theta \sin \varphi \frac{N}{x} \right) J_N(x), \\ w_z &= -\left(\cos \theta \sin \varphi + \sin \theta \cos \varphi \frac{N}{x} \right) J_N(x); & & \\ x &= kR \sin \theta \cos \varphi. \end{aligned} \quad (8)$$

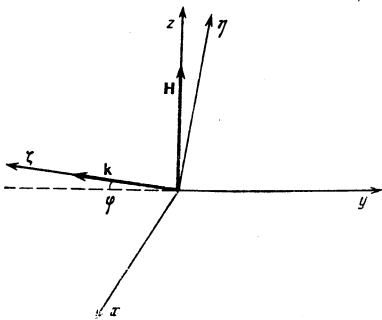


FIG. 1. Coordinate system. The x axis is perpendicular to the plane of the magnetic field \mathbf{H} and the wave vector \mathbf{k} . The ζ axis is parallel to \mathbf{k} and makes an angle $\pi - \varphi$, where $\varphi \ll 1$, with the y axis.

The asterisk in (7) stands for the complex conjugate; $J_N(x)$ and $J_N'(x)$ are a Bessel function and its derivative with respect to x . At $\varphi = 0$ Eq. (7) agrees with the expression obtained for the conductivity tensor in Ref. 1, which deals with cyclotron waves. In the case $N = 0$ and $\omega \ll \Omega$ we get from (7) the expression for the conductivity tensor of the discrete-wave problem.²²

We consider hereafter waves near cyclotron resonance, $|v - i(\omega - N\Omega)| \ll \Omega$, with wavelength much shorter than the cyclotron radius of the conduction electrons ($kR \gg 1$). We assume also a strong spatial dispersion of the wave in the \mathbf{H} direction ($|\omega - N\Omega| \ll k_z v$). The opposite limiting case corresponds to cyclotron waves.¹ In addition we assume that $k_z v \ll \Omega$; then, given the value of ω , the imaginary part of the denominator in (7) vanishes only at one value of N , and we can confine ourselves in the sum over N to this resonant term. Taking into account all the inequalities presented above we can write

$$|v - i(\omega - N\Omega)| \ll k_z v \ll \Omega \ll kv. \quad (9)$$

Whence, in particular, it follows that $\varphi \ll (kR)^{-1}$ ($k_x = 0, k_y \approx -k, k_z \approx \varphi k$).

We calculate now an asymptotic expression for the conductivity tensor under these conditions. Thus, out of the entire sum over N we retain in σ_{ij} only the resonant term. We note here that by virtue of (9) the resonance takes place at $\cos \theta \ll 1$, so that the Bessel-function argument $x \gg 1$ and we can use for these functions their asymptotic expansions.²⁴ Integrating next in (7) with respect to θ , we get after cumbersome calculations

$$\sigma_{ij} = \sigma_0 \begin{pmatrix} F_0 - (-1)^N F_1 & (-1)^N (G_0 - uG_1) & -\beta(-1)^N G_1 \\ -(-1)^N (G_0 - uG_1) & u & \beta(1 - uK) \\ \beta(-1)^N G_1 & \beta(1 - uK) & \beta(2\alpha\varphi - \beta K) \end{pmatrix}. \quad (10)$$

Here

$$\begin{aligned} \sigma_0 &= 3n_0 e^2 / 2m\alpha^2 \Omega \varphi, & u &= (v - i\omega + iN\Omega) / k_z v, \\ \alpha &= kR, & \beta &= (v - i\omega) / kv, & K &= 1 + (-1)^N F_1; \end{aligned}$$

$|u| \ll 1$ according to (9). Next

$$F_0 = \frac{1}{\pi} \int_0^\pi d\theta \frac{\sin^2 \theta}{u + i \cos \theta} = (1 + u^2)^{-1/2} - u \approx 1 - u + \frac{u^2}{2} \quad (11)$$

(see, e.g., Ref. 25 concerning the method of integrating F_0)

$$G_0 = \frac{1}{\pi} \int_0^\pi d\theta \sin \theta \cos(2\alpha \sin \theta) = (\pi\alpha)^{-1/2} \cos(2\alpha - \pi/4). \quad (12)$$

The integration was by the stationary-phase method

$$\begin{aligned} F_1 &= \frac{1}{\pi} \int_0^\pi d\theta \sin^2 \theta \frac{\sin(2\alpha \sin \theta)}{u + i \cos \theta} \\ &= \sin(2\alpha + w^2) - \sqrt{2} [\cos \psi C(w) + \sin \psi S(w)], \\ G_1 &= \frac{1}{\pi} \int_0^\pi d\theta \sin \theta \frac{\cos(2\alpha \sin \theta)}{u + i \cos \theta} \\ &= \cos(2\alpha + w^2) + \sqrt{2} [\sin \psi C(w) - \cos \psi S(w)], \end{aligned} \quad (13)$$

where

$$\psi = 2\alpha + w^2 - \pi/4, \quad w = u\alpha^{1/2}, \quad w \ll \alpha^{1/2};$$

$$S(w) = \left(\frac{2}{\pi}\right)^{1/2} \int_0^w \sin t^2 dt, \quad C(w) = \left(\frac{2}{\pi}\right)^{1/2} \int_0^w \cos t^2 dt;$$

$S(w)$ and $C(w)$ are Fresnel integrals.

The integration of F_1 and F_2 was approximate. By changing to a new variable $\gamma = \alpha^{1/2} \cos \theta$, we reduce the expressions for F_1 and G_1 to integrals that are expressed,²⁶ after replacing the upper limit by infinity, in terms of the probability integral $\Phi(w\sqrt{i})$. In addition, it was assumed that $\alpha \sin \theta \approx \alpha - \gamma^2/2$. The calculations in (13) are accurate to u^2 .

From (10), (11), and (13) it follows that the real part of σ_{xx} , which is mainly responsible for the wave damping, has an oscillating term $1 - (-1)^N \sin(2\alpha + w^2)$ that describes the magnetic Landau damping^{21,27} and vanishes at

$$\alpha^{1/2} + w^2 = \alpha_n = \pi[n + 1/4(-1)^N], \quad n=1, 2, 3, \dots \quad (14)$$

The mechanism of such Landau-damping oscillations of electromagnetic waves propagating at an angle to the magnetic field was first described by Kaner and Skobov²¹ and is essentially analogous to the geometric resonance in the damping of ultrasound in a metal in a magnetic field.²⁸

We now dwell on the physical meaning of the parameter w . The main contribution to σ_{xx} is made by resonant electrons, i.e., those for which the denominator of the integrand in (7) vanishes. Finding $\nu - i(\omega - N\Omega)$ from this condition we have, in accord with the definition of w , $w^2 = (v/v)^2 kR$. Hence

$$kR + w^2/2 = kR(1 - v_s^2/2v^2).$$

Under condition $v_s/v \ll 1$ the factor

$$R(1 - v_s^2/2v^2) = R_1,$$

where R_1 is the cyclotron radius of the electrons from a noncentral section of the Fermi surface. In this case R_1 characterizes the resonant electrons. Consequently $k(R - R_1) = w^2/2$, i.e., the parameter w is a measure of the distance from the Fermi-surface section of the resonant (effective) electrons and the central section. In particular, the condition $|w| \ll 1$ means that $R - R_1 \ll k^{-1}$. According to (19), $|w| \ll \alpha^{1/2}$, and then $R - R_1 \ll R$.

We consider hereafter waves near the minimum of their damping, i.e., at $\alpha \approx \alpha_n - w^2/2$. We then obtain from (10), taking (11)-(13) into account, the following expression for the two-dimensional components of the conductivity tensor $\bar{\sigma}_{\alpha\beta}$ (5):

$$\sigma_{xx} = \sigma_0 [\xi - \eta \alpha' + i(\rho \alpha_n^{-1/2} - P + Q^2 f)], \quad (15)$$

$$\sigma_{xy} = -i\sigma_0(\rho \alpha_n^{-1/2} - f), \quad \sigma_{yx} = \sigma_0(g - Qf), \quad \sigma_{zz} = -\sigma_{yy},$$

where

$$\xi = 2 \sin^2(\alpha - \alpha_n - \rho^2/2), \quad w = \eta - i\rho, \quad (16)$$

$$\eta = (v - \Gamma N \Omega) / \varphi \alpha_n^{1/2} \Omega, \quad \rho = (\omega_0 - N \Omega) / \varphi \alpha_n^{1/2} \Omega,$$

$\omega = \omega_0(1 - i\Gamma)$, Γ is the relative damping of the wave. We assume in η at $N \neq 0$ that $\omega_0 \approx N\Omega$. Thus, ρ is a spectral characteristic of the wave, and η describes the damping. Finally,

$$g = -(a/2 - \rho Q) \alpha_n^{1/2}, \quad a = 2\pi^{-1/2} \sin(\rho^2 - \pi/4), \quad a' = a - 2\rho Q.$$

In (15) we have used also in the assumption that $\rho\eta \ll 1$. The Fresnel integrals are then readily resolved into their real and imaginary parts:

$$S(w) = iS(\rho) - \eta(2/\pi)^{1/2} \sin \rho^2, \quad C(w) = -iC(\rho) + \eta(2/\pi)^{1/2} \cos \rho^2, \\ P = C(\rho) - S(\rho), \quad Q = C(\rho) + S(\rho), \quad f = N/2\varphi\alpha^2.$$

We consider the case $f \ll 1$, and neglect therefore in (15) the terms of higher order in f . In addition, we neglect $\eta\alpha_n^{-1/2}$ compared with η . From the condition for f and from the inequalities in (9) we have $N/2\alpha^2 \ll \varphi \ll \alpha^{-1}$.

SPECTRUM, POLARIZATION, DAMPING

Now, substituting the expressions for the conductivity-tensor $\bar{\sigma}_{\alpha\beta}$ (15) in the dispersion equation (4), we obtain for its real part

$$X^2 - X[P - (1+Q^2)f] - \frac{\rho^2}{\alpha_n} + \frac{\rho}{\alpha_n^{1/2}} P - g^2 - \left[P - 2gQ + \frac{\rho}{\alpha_n^{1/2}} (Q^2 - 1) \right] f = 0. \quad (17)$$

We have introduced here the symbol $X = k^2 c^2 / 4\pi\omega_0\sigma_0$. Since we have fixed kR , it is convenient to change from k in X to α . In this case

$$X = h^2 \alpha_n^{1/2} / 2\pi^{1/2} (\rho + N/\varphi\alpha_n^{1/2}),$$

where $h^2 = H^2 / 3\pi^{1/2} n_0 \mu v^2$ is the normalized magnetic field ($h \sim \Omega/\omega_p$, ω_p is the plasma frequency of the conduction electrons). Solving (17) for h^2 we get

$$h_{\pm}^2 = \pi^{1/2} (N/\varphi\alpha_n^{1/2} + \rho) \alpha_n^{-1/2} \{ [P - (1+Q^2)f] \pm (L^2 + T^2)^{1/2} \}, \quad (18)$$

where

$$L = 2\rho\alpha_n^{-1/2} - P + (Q^2 - 1)f, \quad T = 2(g - Q^2f).$$

Equation (18) represents the wave spectrum in the form of the dependence of H on ω_0 and α_n .

It is seen that both solutions of (17) are real. However, only values $h^2 > 0$ have a physical meaning. At $N = 1.3$ and $n = 20$ these solutions are shown in Fig. 2. In the numerical calculations it was assumed that $n_0 = 10^{23} \text{ cm}^{-3}$, $v = 1.46 \cdot 10^8 \text{ cm/sec}$, and $\varphi = 4 \cdot 10^{-3}$. The number of the curve on the figure corresponds to the value of N for which this curve was plotted, and the + or - subscript of the number of the curve corresponds to the sign in the curly brackets of (18).

Figure 3 shows the dependence of h_{\pm}^2 on $n(\varphi = 10^{-2}, N$

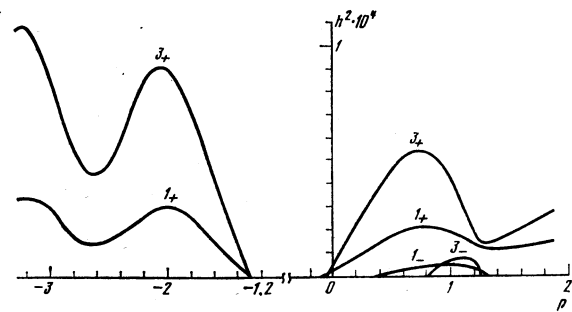


FIG. 2. Spectrum of electromagnetic waves near cyclotron resonance. Plot of $h_{\pm}^2(\rho)$ at fixed N and $n=20$. The number of the curve coincides with the value of N for which the curve was plotted. The index of the number of the curve coincides with the index of the solution.

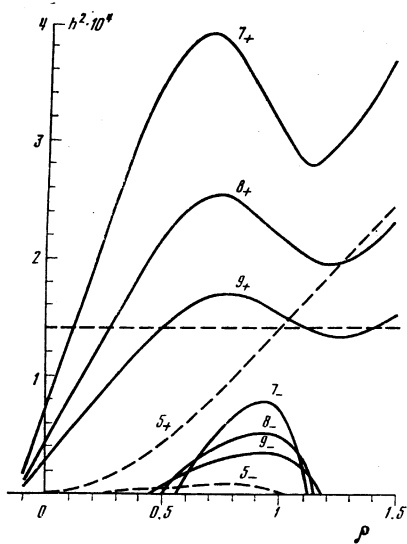


FIG. 3. Spectrum of electromagnetic waves. The solid curve is a plot of $h_{\pm}(\rho)$ at fixed α_n and $N=1$. The number of the curve coincides with the value of n for which the curve was plotted. The index of the number of the curve coincides with the index of the solution. The dashed curve shows the spectrum of the low-frequency waves at $N=0$ and $n=5$. The dashed line is a plot of the field for which the dispersion curve of $\omega_0(k)$ was plotted on Fig. 4.

= 1). Just as in Fig. 2, the index of the number of the curve corresponds to the sign in the curly brackets in (18), but the number of the curve now coincides with the value of n at which this curve was plotted. It is seen that the solution h_{\pm}^2 exists in a limited region of positive values of ρ . It follows from (17) that h_{\pm}^2 becomes positive when the free term of this equation is positive. The positive value of this term determines also the region of negative ρ in which there are no solution $h_{\pm}^2 > 0$. The solution h_{\pm}^2 exists in a wider range of fields and frequencies than h_{\pm}^2 . The spectrum of the wave determined by h_{\pm} consists of two branches, one of which located entirely in the region of negative ρ , i.e., the wave frequency is lower than the cyclotron frequency. The second branch crosses the ordinate axis. This means that the dispersion curve passes through $N\Omega$. Such a singularity of the wave was noted also in Ref. 20.

The solution h_{\pm}^2 oscillates with change of ρ . These oscillations are due to the Hall conductivity $\sigma_{x\eta}$. As already noted, the main contribution to the dissipative conductivity is made by resonant electrons from a non-central section of the Fermi surface. On the other hand, the important role in the Hall conductivity is played by the contribution of electrons from the central section of the Fermi surface. Since we fix $\alpha + \omega^2/2$, the $\sigma_{x\eta}$ term that oscillates as a function of α becomes a function of ρ (15). In Eq. (18) the oscillations are described by the function g . The amplitude of the oscillations decreases with increasing ρ and depends on N and n . It increases with increasing N and decreases with n .

We present now the spectrum of the wave in the form of a function ω_0 of k at a fixed magnetic field H . From the definition (16) of ρ we can obtain

$$\omega_0 = N\Omega [1 + \varphi \alpha_n^{1/2} N^{-1} \rho(H, \alpha_n, \varphi)], \quad (19)$$

where ρ is already a function of H , α_n , and φ and should be determined from (18). At fixed H and φ this can yield $\rho(\alpha_n)$ and then, using (19) and (14), we can easily plot $\omega(k)$, as shown in Fig. 4, in the coordinates $(\omega - \Omega)/\Omega$ and kR . The dispersion curve was plotted at $H = 4.25 \cdot 10^4$ Oe and $\varphi = 10^{-2}$. This value of the field H is shown in Fig. 3 by a dashed line parallel to the abscissa axis. The abrupt change of the slope of the dispersion curve is due to the ambiguity of ρ at the given H (Fig. 3). The steep section of the curve is plotted at one value of α_n , and the entire dispersion is due to the change of ρ . In those cases when H falls in the interval where ρ is single-valued in the region of the allowed values, there is no steep section on the dispersion curve. As can be seen from Fig. 3, this is valid, for example, at $h^2 = 1.8 \cdot 10^{-4}$. The distinguishing features noted here are typical of all the spectrum branches determined by h_{\pm} . The function $\omega_0(k)$ for the h_{-} wave is more complicated. At lower frequencies and small $H \sim 10^3$ Oe ($h^2 \sim 10^{-5}$) this wave was negative dispersion.

The electric field in the waves considered is directed mainly along k :

$$E_t = -(iQE_x + E_n)/2\varphi\alpha, \quad (20)$$

whence $E_z \gg E_x, E_n$. The electric field components transverse to k are connected by the relation

$$E_n = -iD_{\pm}E_x, \quad (21)$$

where the polarization coefficient D_{\pm} is given by

$$D_{\pm} = (X_{\pm} + \rho\alpha_n^{-1/2} - P + Q^2f)/(g - Qf); \quad (22)$$

$$X_{\pm} = X(h_{\pm}).$$

The character of the dependence of D_{\pm} on ρ is shown in Fig. 5 for $n=20$ and $N=1$. For the waves determined by h_{+} , $D_{+} > 0$ and for the h_{-} wave the polarization coefficient $D_{-} < 0$, i.e., h_{+} and j_{-} describe right- and left-polarized waves. The broad minimum of D_{+} at $\rho > 0$ occurs in the region where the h_{-} wave exists. The oscillations of D_{+} as a function of ρ , just as the oscillations in the spectrum, are due to $\sigma_{x\eta}$.

When (15) is substituted in its imaginary part the dispersion equation (4), takes the form

$$\eta a' - \xi = 0. \quad (23)$$

This yields for the relative damping Γ

$$\Gamma = \frac{\nu}{N\Omega} - \frac{2\varphi\alpha_n^{1/2}}{Na'} \sin^2\left(\alpha - \alpha_n - \frac{\rho^2}{2}\right); \quad (24)$$

a' was defined earlier. This is an even and negative

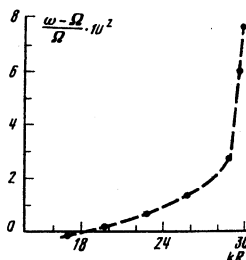


FIG. 4. Spectrum of electromagnetic waves. Plot of $\omega_0(k)$ at $N=1$ and constant H . The points are the values of ω_0 at $kR = \alpha_n + \rho^2/2$.

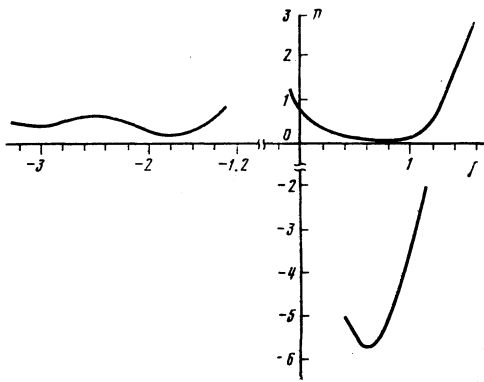


FIG. 5. Dependence of the polarization of the electric field in the electromagnetic wave on ρ at $N=1$ and $n=20$.

function of ρ : when $|\rho|$ is increased, a' increases monotonically.

We consider now limiting cases. Under the condition $|\rho| \ll 1$ Eq. (17) simplifies. Retaining in it the principal terms in ρ and α^{-1} , we get

$$X^2 - X \left[\frac{2}{\pi} \rho - f \right] - (2\pi\alpha)^{-1} = 0. \quad (25)$$

At $\rho \ll 1$ we have $P \approx Q \approx (2/\pi)^{1/2} \rho$. Expressing ρ [from (25)] and substituting the result in (19), we obtain for the wave spectrum the result of Blank and Kaner²⁰

$$\omega_0 = N\Omega \left[1 + \left(\frac{\Omega c \Phi}{\omega_p v N} \right)^2 \alpha_n^{-1/2} - \frac{1}{4} \left(\frac{\tilde{\omega}_p v}{\Omega c} \right)^2 \alpha_n^{-1/2} + \left(\frac{\pi}{8} \right)^{1/2} \alpha_n^{-1/2} \right]. \quad (26)$$

Here $\tilde{\omega}_p = (9/2\pi)^{1/4} \omega_p$. For the damping Γ we readily obtain from (24)

$$\Gamma = \frac{\nu}{N\Omega} + \frac{\Phi(2\pi\alpha_n)^{1/2}}{N} \sin^2(\alpha - \alpha_n),$$

which also agrees with the result of Ref. 20.

When ρ tends to zero we have $a' \approx -(2/\pi)^{1/2}$. In the other limiting case $\rho \gg 1$ we can neglect the renormalization in $\tilde{\sigma}_{\alpha\beta}$ ($f \approx 0$), and in addition $P \approx 0$ and $|Q| \approx 1$ accurate to ρ^{-1} . Taking this into account, it follows from (15) that all the components $\sigma_{\alpha\beta}$ in the real part of the dispersion equation (4) are of the same order, and σ_{xx} and $\sigma_{\eta\eta}$ are equal in magnitude and opposite in sign. The coefficient of k^2 in (4) is then zero and the solutions of the dispersion equation, which are equal but opposite, are determined by the free term $\sim (\sigma_{xx}\sigma_{\eta\eta} + \sigma_{xn}^2)$. According to (18) we obtain for these solutions

$$X = \pm \rho \alpha^{-1/2}. \quad (27)$$

Substituting (27) in (19), we obtain for the wave spectrum

$$\omega_0 = N\Omega \left[1 \pm \frac{2}{3\sqrt{2}} \left(\frac{c\Phi}{\omega_p \Omega N} \right)^2 v^2 k^2 \right]. \quad (28)$$

Accurate to a coefficient 2/3, the expression for the spectrum of the wave with $\omega_0 > N\Omega$ agrees with the result of Aronov and Kaner¹⁾,¹⁸ where the wave was connected with $\sigma_{\eta\eta}$. We note that in Refs. 18 and 20 they investigated the same wave but for different limiting cases.

Equation (18) describes also the spectrum of the low-frequency waves. At $N=0$ we get from (18)

$$h_{\pm}^2 = \pi^{1/2} \rho \alpha_n^{-1/2} \{ P \pm [(2\rho \alpha_n^{-1/2} - P)^2 + 4g^2]^{1/2} \}. \quad (29)$$

This expression differs analytically from the analogous expression previously obtained in Ref. 23, where $F_0 \approx 1$ was assumed. This difference, however, leads only to a numerical difference between the results; all the spectrum singularities noted in Ref. 23 remain here, too. A plot of the function $h_{\pm}^2(\rho)$ corresponding to (29) is shown dashed in Fig. 3. No oscillations of h_{\pm}^2 appear in this case, since they are suppressed by the stronger dependence on ρ in the factor preceding the curly brackets in (29).

CONCLUSION

The equation obtained for the spectrum of electromagnetic waves propagating at an angle to the magnetic field thus describes waves near the cyclotron resonance as well as low-frequency ($\omega \ll \Omega$) waves at $N=0$. Three waves exist near cyclotron resonance. One was investigated earlier in the limiting cases $|w| \gg 1$ and $|w| \ll 1$. It is considered in this article in the entire region $|w|/\alpha^{1/2} \ll 1$ of the values of w . This wave has right-hand polarization. The two other waves were investigated here for the first time ever. Their polarization coefficients are of opposite sign. The frequencies of the right- and left-polarized waves are smaller and larger than $N\Omega$, respectively.

As already noted, the parameter w is a measure of the distance from the section of the Fermi surface of the effective electrons to the central section. We note, however, that a distinction between these sections is meaningful only if the difference $R - R_1 = R\rho^2/2\alpha$ between their radii is larger than the spread $\Delta R = R(\Delta\theta)^2/2$, of the radii of the effective electrons, which is determined by the width $\Delta\theta = \nu/k_z v$ of the maximum of the resonance curve $[\nu - i(\omega - N\Omega - k_z v \cos\theta)]^{-1}$ in (7), i.e., if $\nu/k_z v < \rho\alpha^{-1/2}$. This inequality leads to $\nu < |\omega_0 - N\Omega|$. In the opposite case the sections R and R_1 do not differ and then (14) takes the form $\alpha = \alpha_n$. At $|w| \ll 1$, even if $\nu < |\omega_0 - N\Omega|$, presence of w^2 in (14) is immaterial and consequently at small $|w|$ the results obtained here do not depend on the ratio of ν and $|\omega_0 - N\Omega|$.

Thus, from the data on the electromagnetic waves in the case $\nu < |\omega_0 - N\Omega|$ we can obtain information on the non-extremal sections of the Fermi surface of the conduction electrons. The most convenient for observation are right-polarized waves in the field and frequency region in which $|w| \sim 1$, i.e., for example, at $H \sim 5 \cdot 10^4$ Oe, $\varphi \sim 10^{-2}$, $kR \approx 20$, $\omega - \Omega \approx 0.05\Omega$.

¹⁾The absence of N from the denominator of the right-hand side of the equation for the wave spectrum in Ref. 18 is apparently the result of a misunderstanding.

¹⁾É. A. Kaner and V. G. Skobov, Fiz. Tverd. Tela (Leningrad) **6**, 1104 (1964) [Sov. Phys. Solid State **6**, 851 (1964)].

²⁾M. Ya. Azbel' and É. A. Kaner, Zh. Eksp. Teor. Fiz. **32**, 896 (1957) [Sov. Phys. JETP **5**, 730 (1957)].

³⁾M. C. Steele and B. Viral, Wave Interactions in Solid State Plasmas, McGraw, 1969. Russ. transl. Atomizdat, 1973, p. 104.

⁴⁾P. M. Platzman and P. A. Wolff, Waves and Interactions in Solid State Plasmas, Academic, 1972. Russ. transl. Mir, 1975, p. 104.

- ⁵E. A. Kaner and V. G. Skobov, *Usp. Fiz. Nauk* **89**, 367 (1966) [*Sov. Phys. Usp.* **9**, 480 (1967)].
- ⁶E. A. Kaner and V. G. Skobov, *Adv. Phys.* **17**, 605 (1968).
- ⁷J. Mertsching, *Phys. Status Solidi* **26**, 9 (1968).
- ⁸V. Ya. Demikhovskii and A. P. Protogenov, *Usp. Fiz. Nauk* **118**, 101 (1976) [*Sov. Phys. Usp.* **19**, 53 (1976)].
- ⁹T. D. Kaladze, D. G. Lominadze, and K. N. Stepanov, *Fiz. Tverd. Tela (Leningrad)* **15**, 119, 3312 (1973) [*Sov. Phys. Solid State* **15**, 80 (1973), 2206 (1974)].
- ¹⁰K. Saermark and J. Lebeck, *Phys. Status Solidi B* **65**, 543 (1974); **72**, 375, 631 (1975).
- ¹¹J. Lebeck and K. Saermark, *Phys. Lett.* **A54**, 468 (1975).
- ¹²J. B. Frandsen, L. -E. Hasselberg, J. Lebeck, and K. Saermark, *Phys. Status Solidi B* **67**, 501 (1975).
- ¹³E. A. Kaner, V. L. Fal'ko, and V. A. Yampol'skii, *Zh. Eksp. Teor. Fiz.* **71**, 2389 (1976) [*Sov. Phys. JETP* **44**, 1260 (1976)].
- ¹⁴K. Saermark, J. Lebeck, and H. Johansen, *Phys. Status Solidi B* **83**, 187 (1977); *J. Phys. F. Met. Phys.* **7**, 2121 (1977); **8**, 2145 (1978).
- ¹⁵E. A. Kaner, I. M. Makarov, V. L. Fal'ko, and V. A. Yampol'skii, *Fiz. Nizk. Temp.* **3**, 1427 (1977) [*Sov. J. Low Temp. Phys.* **3**, 686 (1977)].
- ¹⁶R. A. Gordon and J. B. Frandsen, *Solid State Commun.* **24**, 221 (1971).
- ¹⁷M. Ya. Azbel' and E. A. Kaner, *Zh. Eksp. Teor. Fiz.* **39**, 80 (1960) [*Sov. Phys. JETP* **12**, 58 (1960)].
- ¹⁸I. E. Aronov and E. A. Kaner, *Fiz. Nizk. Temp.* **2**, 1277 (1976) [*Sov. J. Low Temp. Phys.* **2**, 622 (1976)].
- ¹⁹I. E. Aronov and E. A. Kaner, *Fiz. Nizk. Temp.* **4**, 76 (1978) [*Sov. J. Low Temp. Phys.* **4**, 38 (1978)].
- ²⁰A. Ya. Blank and E. A. Kaner, *Phys. Status Solidi* **22**, 47 (1967).
- ²¹E. A. Kaner and V. G. Skobov, *Zh. Eksp. Teor. Fiz.* **45**, 610 (1963) [*Sov. Phys. JETP* **18**, 419 (1963)].
- ²²E. A. Kaner and V. G. Skobov, *Physics* **2**, 165 (1966).
- ²³R. G. Khlebopros, L. M. Gorenko, and Yu. I. Man'kov, *Zh. Eksp. Teor. Fiz.* **67**, 1447 (1974) [*Sov. Phys. JETP* **40**, 720 (1974)].
- ²⁴E. Jahnke, F. Emde, and F. Loesch, *Special Functions* (Russ. transl., Nauka, 1964), p. 223.
- ²⁵M. A. Evgrafov, *Analiticheskie funktsii (Analytic Functions)*, Nauka, 1968, p. 253.
- ²⁶I. S. Gradshteyn and I. M. Ryzhik, *Tablitsy integralov, summ, ryadov i proizvedenii (Tables of Integrals, Sums, Series, and Products)*, Nauka, 1962, p. 352 [Pergamon, 1963].
- ²⁷G. A. Vugalter and V. Ya. Demikhovskii, *Zh. Eksp. Teor. Fiz.* **70**, 1419 (1976) [*Sov. Phys. JETP* **43**, 739 (1976)].
- ²⁸A. B. Pippard, *Philos. Mag.* **2**, 1147 (1957).

Translated by J. G. Adashko

Observation of the refraction of conduction-electron trajectories by an intercrystal boundary in aluminum

Yu. V. Sharvin and D. Yu. Sharvin

Institute of Physics Problems, USSR Academy of Sciences
(Submitted 28 June 1979)
Zh. Eksp. Teor. Fiz. **77**, 2153-2156 (November 1979)

A radio-frequency size effect (RSE) was observed in bicrystalline aluminum plates with a twin boundary parallel to the outer surface. The positions and amplitudes of the RSE lines attest to a high transparency of the twin boundary to electrons, and indicates that the tangential component of the quasimomentum is conserved when this boundary is crossed.

PACS numbers: 61.70.Ng, 72.15.Qm

The interaction of conduction electrons with intercrystal boundaries was previously revealed in experiment by its averaged effect on the electric conductivity of polycrystals of pure metals (see, e.g., Refs. 1 and 2). It is obviously of interest to develop experimental methods with which to observe the scattering and diffraction of various groups of electrons by intercrystal boundaries of various types.

We have attempted for this purpose to observe the radio-frequency size effect (RSE) in the geometry indicated above. It can be assumed that in this case one can observe the lines of the ordinary RSE in each of the crystals, as a result of diffuse scattering of the electrons by the boundary as well as lines of the RSE due to the presence of electron trajectories that are refracted on passing through the boundary.

Planar intercrystalline boundaries were obtained by annealing (one hour at 650 C) aluminum samples mea-

suring $1 \times 1 \times 2$ cm with a resistance ratio $R_{293K}/R_{4,2K} = 3 - 5 \cdot 10^3$. Prior to annealing the samples were cooled in liquid nitrogen and subjected to 3-4% deformation. In approximately half the samples etching has revealed, besides the more or less bent boundaries between arbitrarily oriented crystals, also twin boundaries directed along the (111) planes of bordering crystals obviously produced from one seed. Measurements under a microscope revealed no visible deviations of these boundaries from a plane (accurate to 3-5 μ m) over the entire perimeters of the boundaries, which in some cases passed through the entire sample.

A sample containing a twin boundary was mounted on an electric-spark cutting machine in such a way that the cutting plane was parallel to the twin plane, and single-crystal and bicrystal plates of equal thickness were cut from the crystal. After chemical polishing we measured the thickness of the single crystal and the bicry-